Modelling of Alfvén cascades in NBI heated stellarator plasmas

Allah Rakha[1], M.J. Mantsinen[1, 2], A.V.Melnikov[3, 4], S.E. Sharapov[5],
D.A.Spong[6], A. López-Fraguas[7], F. Castejón[7], J.L. dePablos[7]
[1]*Barcelona Supercomputing Center (BSC), 08034, Barcelona, Spain,*
[2]*ICREA, Pg. Lluís Companys 23, 08010 Barcelona, Spain,*
[3]*National Research Center 'Kurchatov Institute', 123182, Moscow, Russia,*
[4]*National Research Nuclear University MEPhI, 115409, Moscow, Russia,*
[5]*CCFE, Culham Science Centre, OX14 3DB, UK,*
[6]*Oak Ridge National Laboratory, TN, 37831, USA,*
[7]*Fusion National Laboratory, CIEMAT, 28040, Madrid, Spain*

Introduction

In magnetic fusion devices with a reversed magnetic shear (RS) configuration, the Alfvén eigenmodes (AEs) called reversed shear Alfvén eigenmodes (RSAE) or Alfvén cascades (ACs) [1-2] can be excited by energetic ions enhancing fast-ion re-distribution and losses. ACs were first observed on JT-60U [3] and later investigated and interpreted on JET [4]. ACs have been useful in MHD spectroscopy to determine the exact values of the safety factor (q) in tokamaks [5-6] and the rotational transform, i.e. the iota (ι) in 3D stellarators [7-8]. ACs typically exhibit a quasiperiodic pattern of frequency sweeping. AEs with similar frequency sweeping coherent structures have been recently observed in the TJ-II stellarator (R_0 = 1.5 m; a ≤ 0.2 m; and B_0 = 1 T) [9]. An example is shown in Fig. 1 where pronounced downward frequency sweeping of AEs from 150 kHz down to 25 kHz is observed around t = 1170 ms in discharge 27804.The modes are measured to be located around a normalized minor radius of ρ~0.7 [9]. This observed fast frequency sweeping at a nearly constant line averaged density is expected due to the variations in the iota profile. A simple model proposed in [9] suggests that the variations in an iota profile may appear due to the variations plasma current.

This paper studies the effect of the iota profile shape on the properties of these NBI driven frequency sweeping AEs in TJ-II stellarator using numerical modelling and compares the simulation results with the experimental findings. In this work, we use STELLGAP [10] and AE3D [11] codes based on reduced MHD model for three-dimensional toroidal plasmas [12]. In particular, we simulate the Alfvén continuum structures and the properties of AEs and compare them with the experimental findings. Our work is continuation of previous work [9] where a simple model was used for the mode frequency evolution, assuming a time-varying

iota profile and an Alfvénic mode character, to estimate the mode numbers m and n and the mode radial location.

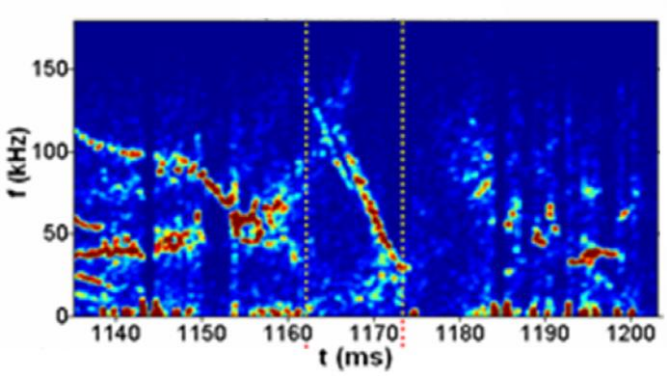

Figure 1: *Frequency sweeping Alfvén eigenmodes (AE) in discharge 27804 in TJ-II stellarator. We focus on the AC observed at t = 1170 ms with fast frequency sweeping and a large frequency range [9].*

Simulation results

In our simulations we have used the experimental plasma density profile for discharge 27804 at t = 1170 ms and we have varied the input rotational transform (iota) profiles to study its effects on the simulated AEs. Figure 2 shows the iota profiles we have considered. The vacuum iota profile is a monotonic iota profile given by the equilibrium code VMEC [13] for discharge 27804 at t = 1170 ms and the non-monotonic (NM) iota profile is based on a simple model presented in [9].

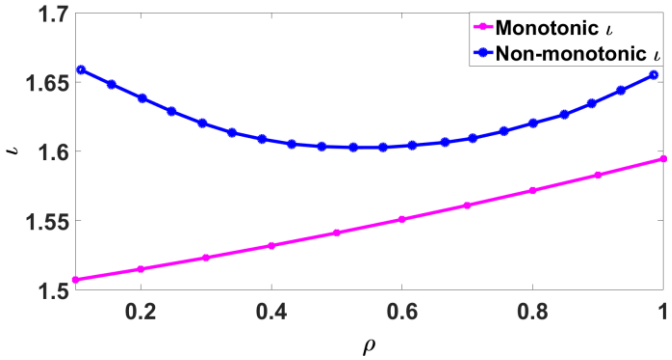

Figure 2*: Rotational transform (iota) profiles employed in simulation, the monotonic iota profiles is the outcome of equilibrium with VMEC [13] code for experimental results of discharge 27804 at t = 1170 ms and non-monotonic (NM) iota profile is proposed based on a simple model presented in [9].*

The shear Alfvén continuum gap structures as given by the STELLGAP code are shown in figure 3. For a monotonic iota profile, a fewer numbers of gaps and extremum points in a smaller frequency and radial range are observed. Simulations also show that Alfvén continuum structures for monotonic iota profile have closed gaps (Fig. 3a), while for non-monotonic iota profile the gaps are relatively open (Fig. 3b). These close/open gaps lead to accommodate different types of AEs and enhance the continuum damping. In case of

non-monotonic iota profile the zero frequency crossings at ρ = 0.55 and ρ =0.9 in the Alfvén continuum are also found as shown in Fig. 3(b).

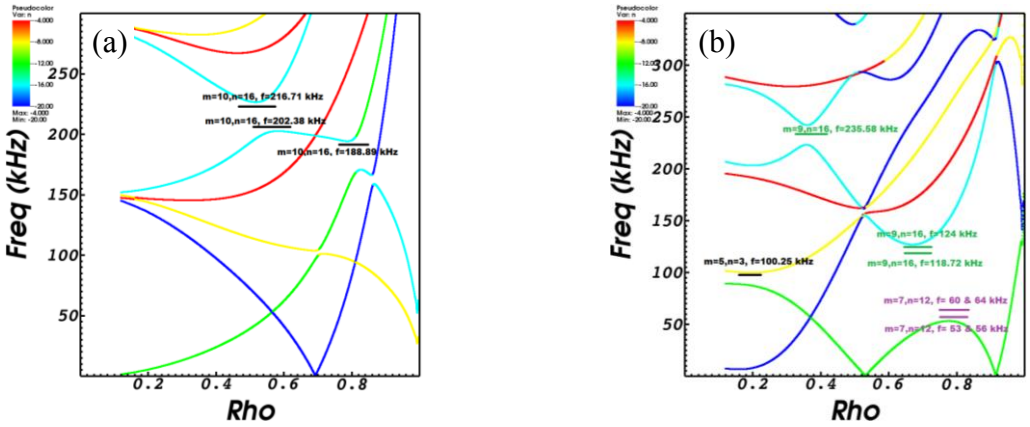

***Figure 3**: Shear Alfvén continuum gap structures of discharge 27804 at t = 1170 ms, (a) for monotonic and (b) for non- monotonic iota profiles. Prominent toroidal mode numbers are shown distinctly with color coding in legends.*

The AE3D simulations for the monotonic iota profile show only one prominent mode (Fig. 4). It has mode numbers m = 10 and n = -16 with three different frequencies of 189, 202 and 217 kHz, located around ρ = 0.80, 0.55 and 0.50 respectively. Their frequencies are higher and their radial localization more inward as compared with the experimentally observed mode. Since in experiments, the mode spans overs a larger range of frequency i.e. 50 kHz to 200 kHz and is radially extended outward around ρ = 0.7.

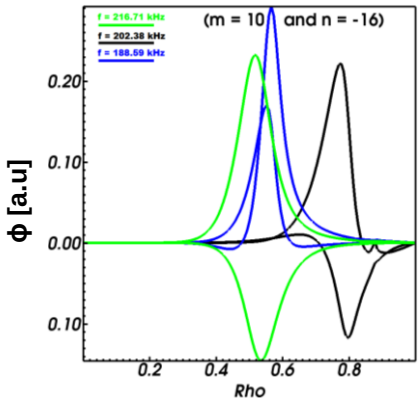

***Figure 4**: Three different frequencies and potential profiles of one modelled AE of the monotonic iota profile for the discharge 27804 at t = 1170 ms. The pronounced combination of toroidal 'n' and poloidal 'm' mode numbers is highlighted in the centre of profiles.*

On the contrary, the AE3D simulations for non-monotonic iota profile show three different prominent AEs covering a larger spectrum of frequency and radially extended relatively outward (Fig. 5). The first of the computed modes is with prominent mode numbers m = 5 and n = -8 and has frequency of 100 kHz and is radially extended over ρ = 0.2. The second mode with m = 9 and n = -16 appears with four different frequencies of 118, 119, 124 and 236

kHz and is radially located around ρ = 0.65, 0.35 respectively. The third mode with m = 7 and n = -12 also have multiple frequencies of 53, 56, 60, and 64 kHz and is radially spread about ρ = 0.8. In non-monotonic iota profile simulations, three different AEs covering a wider range of frequency from 53 to 236 kHz and radially spanned over the wider range, make them more closer with the experimental observations. Their characteristics are broadly consistent with the estimates for the mode numbers and the mode radial locations as given by the simple model employed in earlier work [9].

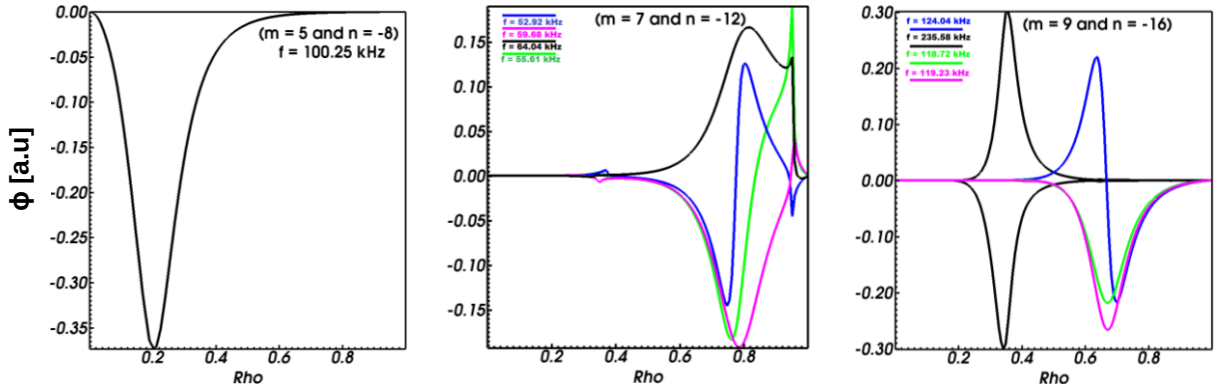

Figure 5: Potential profiles of three modelled AEs for the non-monotonic iota profile for discharge 27804. The modes (m=7, n=-12) and (m=9, n=-16) have four and the mode (m=5, n=-8) has one prominent frequency.

Conclusions The comparison of modelling results between monotonic and non-monotonic iota profiles, and with the experimental findings shows that the non-monotonic iota profile explains better the experimental findings. In our modelling a wide spectrum of modes covering a frequency range from~50 to~250 kHz and located at a normalised minor radius of 0.3-0.7 are found around the position of the iota extremum point roughly consistent with the experimental mode frequency and radial location. If we assume a monotonic ι profile instead, our simulations show a smaller number of modes located at larger minor radii with frequencies covering a narrower range than that observed in the experiment.

This work has been carried out within the framework of the EUROfusion Consortium and has received funding from the Euratom research and training programme 2014-2018 under grant agreement No 633053. The views and opinions expressed herein do not necessarily reflect those of the European Commission. The experimental observations with Russian Scientific Foundation, project 14-22-00193 and it was partly supported by the Competitiveness Programme of NRNU MEPhI.

References

[1] S. E. Sharapov, et al., Physics Letters A 289 (2001)
[2] H. L. Berk et al., Phys. Rev. Lett. 87 (2001) 185002
[3] H. Kimura, et al., Nucl. Fusion 38 1303 (1998)
[4] S. E. Sharapov et al., Phys. Plasmas 9, 2027 (2002)
[5] A. Fasoli, et al., PPCF 44, B159 (2002)
[6] S. E. Sharapov, et al., Nucl. Fusion 46 S868 (2006)
[7] K. Toi, et al., PPCF 53, 024008 (2011)
[8] K. Toi, et al., PRL 105, 145003 (2010)
[9] A. V. Melnikov , et. al, NF 54 123002 (2014)
[10] D. Spong, et al. Phys. Plasmas 10, 3217, (2003)
[11] D.Spong et al Phys. Plasmas 17, 022106, (2010)
[12] S.Kruger, et al, Phys.Plasmas 5, 4169 (1998)
[13] S. P. Hirshman, and J. C. Whitson, Phys. Fluids 26, 3553 (1983)